Empower innovation. Expand capabilities.
Learn how to increase the signal-to-noise ratio and gain flexibility in panel design with the 320-nm laser on the ID7000™ Spectral Cell Analyzer.
Download Tech Note

ID7000™ Spectral Cell Analyzer
SONY

The Journal of Immunology

This information is current as of January 29, 2022.

n-3 Polyunsaturated Fatty Acids Suppress the Localization and Activation of Signaling Proteins at the Immunological Synapse in Murine CD4 $^{+}$ T Cells by Affecting Lipid Raft Formation

Wooki Kim, Yang-Yi Fan, Rola Barhoumi, Roger Smith, David N. McMurray and Robert S. Chapkin

J Immunol 2008; 181:6236-6243; ;
doi: 10.4049/jimmunol.181.9.6236
http://www.jimmunol.org/content/181/9/6236

References This article **cites 48 articles**, 17 of which you can access for free at:
http://www.jimmunol.org/content/181/9/6236.full#ref-list-1

Why *The JI*? Submit online.

- **Rapid Reviews! 30 days*** from submission to initial decision
- **No Triage!** Every submission reviewed by practicing scientists
- **Fast Publication!** 4 weeks from acceptance to publication

**average*

Subscription Information about subscribing to *The Journal of Immunology* is online at:
http://jimmunol.org/subscription

Permissions Submit copyright permission requests at:
http://www.aai.org/About/Publications/JI/copyright.html

Email Alerts Receive free email-alerts when new articles cite this article. Sign up at:
http://jimmunol.org/alerts

The Journal of Immunology is published twice each month by
The American Association of Immunologists, Inc.,
1451 Rockville Pike, Suite 650, Rockville, MD 20852
Copyright © 2008 by The American Association of Immunologists All rights reserved.
Print ISSN: 0022-1767 Online ISSN: 1550-6606.

Downloaded from http://www.jimmunol.org/ by guest on January 29, 2022

n-3 Polyunsaturated Fatty Acids Suppress the Localization and Activation of Signaling Proteins at the Immunological Synapse in Murine CD4$^+$ T Cells by Affecting Lipid Raft Formation[1]

Wooki Kim,* Yang-Yi Fan,* Rola Barhoumi,†‡ Roger Smith,§ David N. McMurray,*†‡¶ and Robert S. Chapkin[2]*†‡

The molecular properties of immunosuppressive n-3 polyunsaturated fatty acids (PUFA) have not been fully elucidated. Using CD4$^+$ T cells from wild-type control and *fat-1* transgenic mice (enriched in n-3 PUFA), we show that membrane raft accumulation assessed by Laurdan (6-dodecanoyl-2-dimethyl aminonaphthalene) labeling was enhanced in *fat-1* cells following immunological synapse (IS) formation by CD3-specific Ab expressing hybridoma cells. However, the localization of protein kinase Cθ, phospholipase Cγ-1, and F-actin into the IS was suppressed. In addition, both the phosphorylation status of phospholipase Cγ-1 at the IS and cell proliferation as assessed by CFSE labeling and [^{3}H]thymidine incorporation were suppressed in *fat-1* cells. These data imply that lipid rafts may be targets for the development of dietary agents for the treatment of autoimmune and chronic inflammatory diseases. ***The Journal of Immunology,*** **2008, 181: 6236–6243.**

The Singer and Nicolson lipid bilayer model of the plasma membrane (1) has evolved significantly to include specialized microdomains, i.e., lipid rafts. Lipid rafts can be classified as morphologically featureless, detergent-resistant membranes due to their insolubility in cold nonionic detergents (2). Their highly enriched cholesterol and sphingolipid content suggests that these membranes are in a liquid ordered (l_o) state, whereas the bulk membrane is in a liquid disordered (l_d) state (3). The biochemical characterization of lipid rafts has provided new insight into the regulation and function of plasma membrane proteins. For example, it is now known that T cell intracellular signaling cascades, endocytosis, protein trafficking, and cell-cell communication are modulated in part by altering the lipid-protein composition of the bulk membrane and specialized lipid microdomains (3–6).

Dietary fish oil, rich in n-3 polyunsaturated fatty acids (PUFA)[3] can alter immune cell function and aid in the resolution of chronic inflammation, e.g., arthritis, Crohn's disease, dermatitis, psoriasis, and ulcerative colitis (7–10). To further investigate the anti-inflammatory properties of fish oil, we have demonstrated that n-3 PUFA modulate CD4$^+$ T cell immune responses in part via reduction in Th1 clonal expansion (11), IL-2 secretion and IL-2R α-chain mRNA transcription (12). However, the molecular mechanisms by which n-3 PUFA suppress CD4$^+$ T cell function are not fully understood.

It has been reported that the fatty acid composition of lipid rafts and the bulk membrane in Jurkat T cells was altered by addition of n-3 PUFA to the culture medium (13). Our lab also demonstrated the modulation of T cell lipid rafts by dietary n-3 PUFA in a mouse model (14). In the latter study, it was demonstrated that dietary fish oil as well as purified docosahexaenoic acid (DHA), a major bioactive n-3 PUFA of 22 carbons and 6 *cis* double bonds (22:6n-3), altered CD4$^+$ T cell plasma membrane fatty acid composition, specifically in phosphatidylserine and phosphatidylethanolamine, which are abundant in the cytofacial leaflet of the cell membrane (15). In contrast, fatty acid profiles in sphingomyelin, phosphatidylinositol, and phosphatidylcholine, which are major lipids in the exofacial leaflet (15) in which TCR is linked, were not altered. These observations may partially explain why n-3 PUFA alter signaling pathways without affecting expression or affinity of the TCR/CD3 complex (16, 17). Furthermore, in complementary studies, changes in lipid raft fatty acid composition were associated with a decrease in the translocation of protein kinase C (PKC)θ, a key molecule regulating CD4$^+$ T cell activation, into lipid rafts in mitogen-stimulated T cells (12). In contrast, n-3 PUFA incubation displaced F-actin, talin, LFA-1α, but not PKCθ from the immunological synapse (IS), where T cells and APC form a conjunction (18). In terms of cell signaling triggered by TCR, it was reported that the scaffold protein CARMA1, the caspase recruitment domain-containing protein 11, is recruited into the IS and plays an essential role in linking Ag recognition, PKCθ activation via translocation into lipid rafts, and NF-κB nuclear translocation (19). From these studies, it is apparent that n-3 PUFA may modulate T cell function via alteration of lipid raft structure and the translocation of signaling molecules.

*Faculty of Nutrition, †Center for Environmental and Rural Health, ‡Department of Veterinary Integrative Biosciences, §Department of Veterinary Pathology, Texas A&M University, and ¶Department of Microbial & Molecular Pathogenesis, Texas A&M University System Health Science Center, College Station, TX 77843

Received for publication July 14, 2008. Accepted for publication August 20, 2008.

The costs of publication of this article were defrayed in part by the payment of page charges. This article must therefore be hereby marked *advertisement* in accordance with 18 U.S.C. Section 1734 solely to indicate this fact.

[1] This work was supported by Grants DK071707, CA59034, and P30ES09106 from the National Institutes of Health (NIH). Confocal and multiphoton microscopy was supported with funding by Grant 1 S10 RR22532-01 from National Center for Research Resources-NIH Shared Instrumentation, performed at the College of Veterinary Medicine & Biomedical Sciences Image Analysis Laboratory, Texas A&M University, College Station, TX.

[2] Address correspondence and reprint requests to Dr. Robert S. Chapkin, Faculty of Nutrition, 321 Kleberg Center, MS 2253, Texas A&M University, College Station, TX 77843-2253. E-mail address: r-chapkin@tamu.edu

[3] Abbreviations used in this paper: PUFA, polyunsaturated fatty acid; IS, immunological synapse; DHA, docosahexaenoic acid; PKC, protein kinase C; MFI, mean fluorescence intensity; GP, generalized polarization; LAT, linker for activation of T cells; PLC, phospholipase C; CTx, cholera toxin; RRI, relative relocation index; WT, wild type.

Copyright © 2008 by The American Association of Immunologists, Inc. 0022-1767/08/$2.00

Downloaded from http://www.jimmunol.org/ by guest on January 29, 2022

We have recently reported that long chain PUFA alter the size and distribution of lipid rafts in HeLa cells, as determined by immunogold electron microscopy (20). These data suggest that plasma membrane organization of inner leaflets is fundamentally altered by n-3 PUFA enrichment. However, to date, the direct visualization of T cell lipid rafts at the IS following n-3 PUFA membrane enrichment has not been reported. Recently, it was demonstrated that the fluorescent probe Laurdan can align itself parallel with the hydrophobic tails of phospholipids in membranes (21–23). Owing to its ability to emit two different wavelengths according to the fluidity of the microenvironment, Laurdan can be used to measure membrane fluidity and visualize lipid rafts in living cells by two-photon microscopy (22).

Because mammals cannot produce n-3 PUFA from the major n-6 PUFA found in the diet due to the lack of Δ15-desaturase activity, it is necessary to enrich the diet with eicosapentaenoic acid (20:5n-3) or DHA to assess their biological properties in vivo. Recently, the *fat-1* gene encoding an n-3 fatty acid desaturase was cloned from *Caenorhabditis elegans* and expressed in mammalian cells (24). This enzyme can catalyze the conversion of n-6 PUFA to n-3 PUFA by introducing a double bond into fatty acyl chains. Hence, transgenic mice expressing *fat-1* allow us to investigate the biological properties of n-3 PUFA without having to incorporate these fatty acids in the diet. Using the *fat-1* mouse model, we report for the first time the effect of n-3 PUFA on 1) the formation of lipid rafts in living $CD4^+$ T cells at the IS, 2) membrane translocation of signaling molecules, 3) phosphorylation (activation status) of key signaling proteins, and 4) the proliferation of $CD4^+$ T cells.

Materials and Methods

Animals, diet, and $CD4^+$ T cell purification

Fat-1 transgenic mice were generated and backcrossed onto a C57BL/6 background by breeding heterozygous mice (24, 25). Littermates were used in all experiments as previously described (25). All procedures followed guidelines approved by the U.S. Public Health Service and the Institutional Animal Care and Use Committee at Texas A&M University. Mice were genotyped using tail DNA. To confirm the phenotype, total lipids were isolated from splenic $CD4^+$ T cells, and the fatty acid profile was characterized by gas chromatography as previously described (14). Animals were fed a 10% safflower oil diet (n-6 PUFA-rich; Research Diets) ad libitum with a 12 h light/dark cycle. The diet contained (per a 100-g diet) 40 g of sucrose, 20 g of casein, 15 g of corn starch, 0.3 g of DL-methionine, 3.5 g of AIN 76A salt mix, 1.0 g of AIN 76A mineral mix, 0.2 g of choline chloride, 5 g of fiber (cellulose), and 10 g of safflower oil. $CD4^+$ T cells from *fat-1* or wild-type (WT) mice were isolated from spleens by a magnetic microbead positive selection method (Miltenyi Biotec) according to the manufacturer's recommendation.

Laurdan labeling

Purified (91.0 ± 1.0% determined by flow cytometry) $CD4^+$ T cells (n = 3) were stained with Laurdan (Invitrogen) for lipid raft visualization. Briefly, 5 μmol/L Laurdan was prepared in serum-free RPMI 1640 medium and incubated with 2×10^6 cells/ml for 30 min at 37°C (21). Cells were subsequently washed and resuspended in serum-free Leibovitz medium. To evaluate the effect of cholesterol depletion on lipid raft formation, cells were pretreated with 10 mmol/L methyl-β-cyclodextrin (Sigma-Aldrich) in fatty acid-free RPMI 1640 medium containing 0.1% BSA for 3 min before Laurdan labeling (26).

$CD4^+$ T cell activation and two-photon microscopy

For mitogenic activation, $CD4^+$ T cells were cocultured with CD3-specifc Ab expressing hybridoma cells (clone 145-2C11, anti-CD3 hybridoma) from the American Type Culture Collection. Coculture was conducted in complete medium (RPMI 1640 medium with 25 mmol/L HEPES (Irvine Scientific)), supplemented with 5% heat-inactivated FBS (Invitrogen), 10^5 U/L penicillin, and 100 mg/L streptomycin (Life Technologies), 2 mmol/L L-glutamine (Glutamax; Life Technologies), and 10 μmol/L 2-ME (Sigma-Aldrich). To validate IS formation, T cells were also incubated with an irrelevant DNP-specific Ab expressing hybridoma cells (clone UC8-1B9, anti-DNP hybridoma) (27). In select experiments, hybridoma cells were prelabeled with Cell Tracker orange-fluorescent tetramethylrhodamine (Invitrogen). Laurdan labeled $CD4^+$ T cells were coincubated with hybridoma cells at a ratio of 5:1. Cell mixtures were seeded onto poly-L-lysine (Sigma-Aldrich) precoated chambered cover glass slides (2×10^6 $CD4^+$ T cells/chamber). After a 30-min incubation period at 37°C, Laurdan was measured by two-photon microscopy (Zeiss LSM 510 META NLO) with a 40X objective 1.3 NA oil at 400–460 and 470–530 nm (Fig. 1, *A–D*) to calculate generalized polarization (GP) values, which indicate l_o and l_d states of the membrane, respectively (22). The Coherent Chameleon femtosecond pulsed Ti:Sapphire laser was set at an excitation of 770 nm.

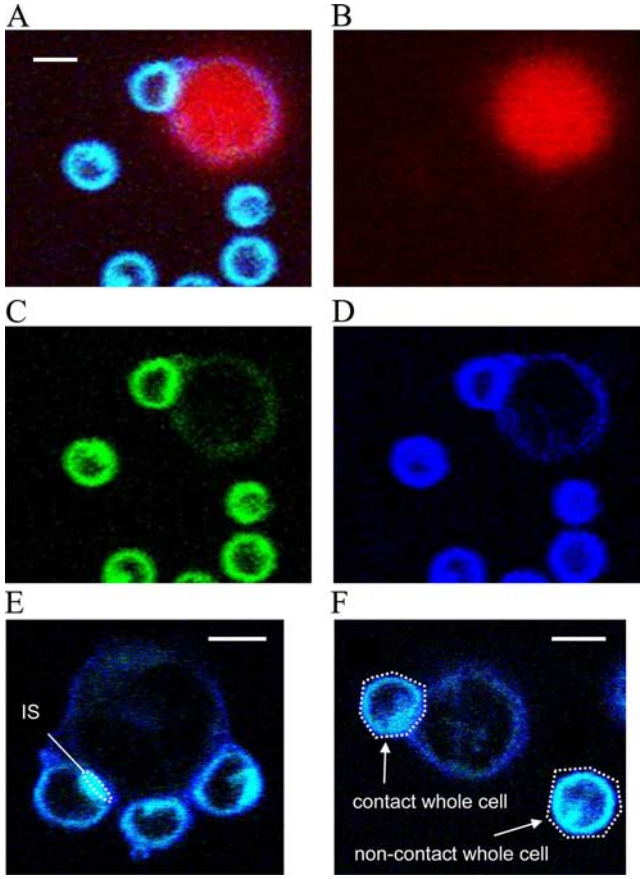

FIGURE 1. Representative two-photon microscopy images of the Laurdan labeled T cells. The 8-bit TIFF format captured images were analyzed in RGB (*A*), red (*B*) (Cell Tracker orange-fluorescent tetramethylrhodamine), green (*C*) ($I_{470-530}$) or blue (*D*) ($I_{400-460}$) channels. Regions of interest (ROI) at T cell IS (*E*) and contact and noncontact whole cell (*F*) were selected by drawing an oval or polygon as shown (white dotted line). Mean intensity from blue and green channels were recorded to calculate GP values as described in *Materials and Methods*. Scale bar represents 5 μm.

GP value calculation

All images were converted to 8-bit/channel TIFF format and were processed using Adobe Photoshop CS3. The mean intensity of each color channel was measured in either whole cells or contact regions of the synapse by drawing a polygon around each cell boundary (whole cell) (Fig. 1*F*) or by drawing an oval at the T cell membrane proximal to the hybridoma cell (Fig. 1*E*). GP value was a ratio obtained by the formula $(I_{400-460} - I_{470-530})/(I_{400-460} + I_{470-530})$, where *I* represents the intensity of each region of interest for the blue and green channels, respectively (21, 22).

Downloaded from http://www.jimmunol.org/ by guest on January 29, 2022

Quantification of protein localization, activation, and GM1 relocation

To assess the relocalization of signaling proteins or cytoskeletal F-actin, isolated $CD4^+$ T cells were mixed with hybridoma cells (5:1) and seeded onto poly-L-lysine precoated cover glass slides. After a 30-min incubation period, cells were fixed in 4% formaldehyde for 20 min, rinsed with PBS, and incubated with 10 mmol/L glycine in PBS for 10 min at room temperature to quench aldehyde groups. Cell membranes were permeabilized by exposure to 0.2% Triton X-100 in PBS for 5 min at room temperature, followed by PBS washing. Cells were subsequently covered with blocking solution (1% BSA/0.1% NaN_3 in PBS) and incubated at 4°C overnight with primary Abs, rabbit Abs specific to either PKCθ (Santa Cruz Biotechnology), linker for activation of T cells (LAT), phospho-LAT (Upstate Biotechnology), CARMA1, phospholipase C (PLC)γ-1, phospho-PLCγ-1 (Cell Signaling Technology) as reported previously (12). After PBS washing, cells were incubated with secondary Alexa Fluor 568 goat Ab to rabbit IgG (Molecular Probes). To visualize F-actin and ganglioside GM1 localization, cells were incubated with F-actin-specific phallotoxin-Alexa Fluor 568 (Molecular Probes) or GM1-specific cholera toxin (CTx) B subunit-FITC (CTx-FITC; Sigma-Aldrich), respectively. Following serial ethanol dehydration steps, samples were mounted onto glass slides with ProLong Antifade reagent (Molecular Probes) (12). Fluorescence images were acquired by confocal microscopy to determine both the translocation and phosphorylation status (activation) of signaling proteins in $CD4^+$ T cells. Either a Bio-Rad Radiance 2000MP multiphoton system (argon laser excitation at 568 nm and emission at 590 nm, 63X objective 1.4 NA water) or Zeiss LSM 510 META NLO nonlinear optics system (argon laser excitation at 543 nm and emission with a longpass 560 nm, 63X objective 1.4 NA oil) was used for image acquisition. Cell images were captured in 8-bit TIFF format, and the percentage of cells with protein patching at the IS was counted to assess the relocalization of signaling proteins or F-actin. GM1 recruitment into the IS was quantified by relative relocation index (RRI) (28). Briefly, polygons were drawn to designate the IS, the contact whole cell and background area. RRI was calculated using mean fluorescence intensity (MFI) in the formula (MFI at the IS background)/(MFI at the contact whole cell background). Quantitative analysis of MFI was performed using Adobe Photoshop CS3 for Windows.

$CD4^+$ T cell proliferation assay

The effect of n-3 PUFA on T cell proliferation was evaluated by the [^{3}H]thymidine incorporation and CFSE labeling as previously described (11, 29). Briefly, 2×10^5 purified $CD4^+$ T cells were stimulated using either control RPMI 1640 complete medium, 5×10^5 anti-CD3 hybridoma cells that were pretreated with 10 μmol/L mitomycin C (Sigma-Aldrich) for 30 min to block cell division, plate-bound CD3-specific mAb (1 ng/L) and soluble CD28-specific mAb (5 ng/L, anti-CD3/28 mAbs; BD Pharmingen) or PMA (1 pg/L) and ionomycin (500 nmol/L) (PMA/ionomycin). Cells were cultured for 72 h in round-bottom 96-well multiplates. For CFSE profile analysis, $CD4^+$ T cells were pretreated with 5 μmol/L CFSE in PBS supplemented with 5% FBS for 10 min (29). After 72 h in culture as described, CFSE was analyzed by flow cytometry (FACSCalibur, BD Biosciences) as previously reported (11). Briefly, cells were harvested by centrifugation and resuspended in PBS. To determine viability, propidium iodide (Sigma-Aldrich) was added to each sample before analysis. CFSE fluorescence was detected using a 530/30 bandpass filter and propidium iodide fluorescence through a longpass 650LP filter. CFSE fluorescence was sufficiently intense to be detected through a 650LP filter. Viable cells were determined using a plot of CFSE vs propidium iodide fluorescence, based on the fluorescence patterns of a sample with CFSE but no propidium iodide. This gate also excluded most of the hybridoma cells because of their higher level of autofluorescence. An additional lymphocyte gate was set based on forward and side light scattering properties. CFSE profiles were analyzed by ModFit LT 3.0 (Verity Software House). Data were expressed as the difference in the percentage (Δpercentage) at each daughter cell generation by calculating (*fat-1* − WT). For the [^{3}H]thymidine incorporation, 4 μCi [^{3}H]thymidine/well (NEN) was added to the cultures for the final 6 h. Cells were harvested using a 96-well cell harvester (Packard Instrument) and thymidine uptake was measured using liquid scintillation counting (Beckman Coulter). Results are expressed as proliferation index, determined by the formula (disintegrations per minute of stimulated wells)/(disintegrations per minute of basal control).

Statistics

Data were analyzed using Student's *t* test to compare *fat-1* and WT cells. Kolmogorov-Smirnov method was applied to test the normality of the data distribution. Statistical interaction of the variables (genotype and regions of interest) was tested by two-way ANOVA. To compare multiple treatment means, one-way ANOVA and LSD multiple posthoc tests were used (SPSS 15.0 for Windows). Data are expressed as mean ± SEM, and differences in data at $p < 0.05$ were considered statistically significant.

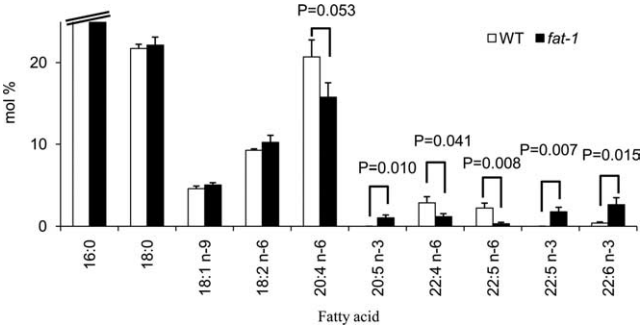

FIGURE 2. Major fatty acid composition of $CD4^+$ T cell total lipids in WT and *fat-1* mice. Splenic $CD4^+$ T cells were isolated from WT or *fat-1* transgenic mice ($n = 5$). Total phospholipids were isolated and fatty acid composition was analyzed by gas chromatography. Mol % was determined using the formula (number of moles of individual fatty acid)/(number of moles of total fatty acids).

Results

n-3 PUFA enhances the formation of lipid rafts at the IS

Both *fat-1* transgenic and WT control offspring were fed a 10% safflower oil diet enriched in n-6 PUFA throughout the duration of

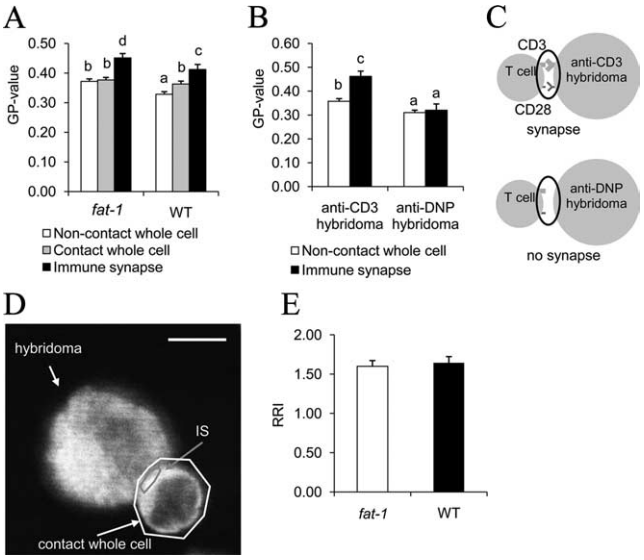

FIGURE 3. Lipid raft formation and GM1 relocalization at the IS of $CD4^+$ T cells. *A*, GP values, which indicate microenvironment fluidity in the plasma membrane, were quantified in $CD4^+$ T cells obtained from either *fat-1* or WT mice (8–14 cells per mouse from 3–4 mice per genotype were examined to obtain a total of $n = 27$–51 observations). Data indicate significant differences at $p < 0.05$ across all treatment groups within experiment. *B*, IS-dependent increase of GP values was confirmed by anti-DNP hybridoma cells (negative control, $n = 6$–9 cells from one mouse per genotype). Data indicate significant differences at $p < 0.05$ across all treatment groups within experiment. *C*, Schematic of IS formation (*top*) and noncontact IS (*bottom*). *D* and *E*, Immunofluorescence analysis of GM1 recruitment into the IS. Purified $CD4^+$ T cells and anti-CD3 hybridomas were coincubated, fixed, permeabilized, and labeled with CTx-FITC. Confocal microscopic images were captured and MFI was measured at the IS relative to the whole cell to calculate RRI, as described in *Materials and Methods*. *D*, Representative image of GM1 localization. Scale bar represents 5 μm. *E*, The relocation of GM1 at the IS was assessed by RRI of CTx-FITC ($n = 31$–32 cells from 3 mice per genotype).

Downloaded from http://www.jimmunol.org/ by guest on January 29, 2022

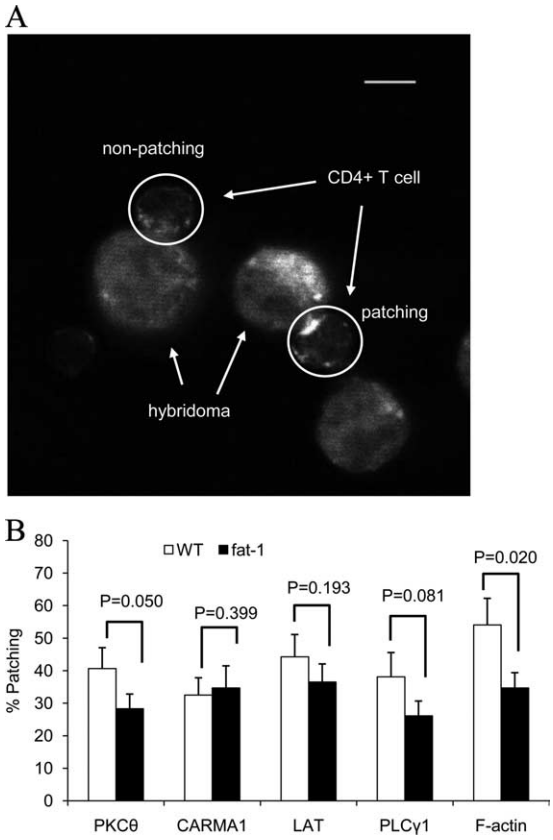

FIGURE 4. Immunofluorescence analysis of localization of signaling molecules into the IS. Purified $CD4^+$ T cells and anti-CD3 hybridomas were coincubated, fixed, permeabilized, and labeled with Abs specific to either PKCθ, CARMA1, LAT, PLCγ-1, or F-actin, as described in *Materials and Methods*. *A*, Representative images of LAT localization to the IS in *fat-1* cells. Image contrast was adjusted. Scale bar represents 5 μm. *B*, Protein localization was assessed by the percentage of patching using (the number of patching cells)/(number of total cells examined), for $n = 37–101$ cells from 2–5 mice per genotype for each protein.

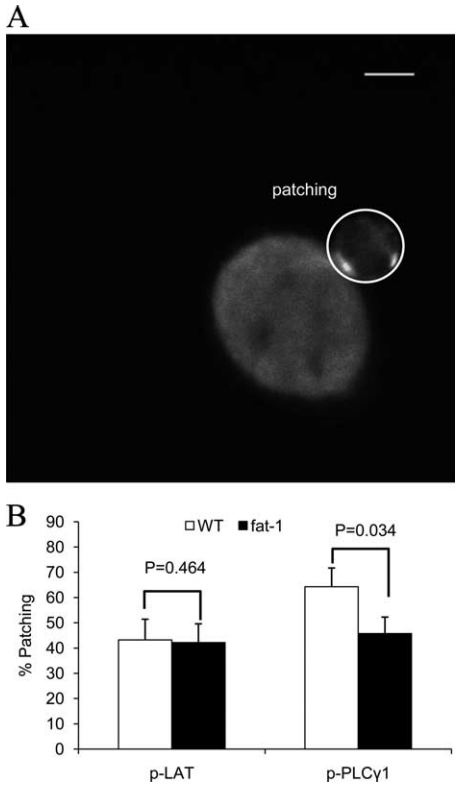

FIGURE 5. Phosphorylation status of signaling proteins at the IS. Purified $CD4^+$ T cells and anti-CD3 hybridomas were coincubated, fixed, permeabilized, and labeled with Abs specific to either phospho-LAT or phospho-PLCγ-1, as described in *Materials and Methods*. *A*, Representative image of LAT phosphorylation at the IS in *fat-1* cells. Image contrast was adjusted. Scale bar represents 5 μm. *B*, Protein activation was assessed by the percentage of patching (for $n = 37–59$ cells from 3–4 mice per genotype for each protein).

study. Splenic $CD4^+$ T cell total lipid fatty acid compositional analyses revealed an increase in n-3 PUFA (eicosapentaenoic acid ($p = 0.010$), docosapentaenoic acid (22:5n-3, $p = 0.007$), and DHA ($p = 0.015$)) and a decrease in n-6 PUFA, specifically arachidonic acid (20:4n-6, $p = 0.053$), adrenic acid (22:4n-6, $p = 0.041$), and docosapentaenoic acid (22:5n-6, $p = 0.008$) in *fat-1* transgenic mice (Fig. 2). In addition, the ratio of n-6 to n-3 PUFA was significantly ($p = 0.003$) suppressed in *fat-1* (5.13 $\pm$ 1.18), compared with WT T cells (35.71 $\pm$ 6.38). These data indicate that an appropriate activity of n-3 fatty acid desaturase was present and that T cells from *fat-1* mice were enriched in n-3 PUFA.

To investigate the effect of endogenous n-3 PUFA on lipid raft formation at the IS, Laurdan labeled $CD4^+$ T cells were cocultured with anti-CD3 hybridoma cells at 37°C in 5% CO_2 for 30 min. Images of conjugate $CD4^+$ T cells and hybridomas were captured, whereas noncontact $CD4^+$ T cells served as a negative control. Two-way ANOVA of GP values revealed that there was no statistical interaction between genotype and regions of interest ($p = 0.430$). GP ratios were significantly ($p < 0.001$, LSD posthoc test) increased at the IS (0.412 $\pm$ 0.017 WT vs 0.452 $\pm$ 0.014 *fat-1*) compared with noncontact T cells (0.329 $\pm$ 0.008 WT vs 0.372 $\pm$ 0.008 *fat-1*) or contact whole cells (0.363 $\pm$ 0.010 WT vs 0.377 $\pm$ 0.008 *fat-1*) (Fig. 3*A*). Overall, raft formation was enhanced in *fat-1* vs WT cells in both resting ($p = 0.016$) and stimulated ($p = 0.022$) $CD4^+$ T cells. The DNP-specific Ab expressing hybridoma was used as a negative control, and failed to exhibit an increase in the GP value at the IS (Fig. 3, *B* and *C*). These data demonstrate that the n-3 PUFA-dependent increase in the GP value is IS-dependent.

In independent experiments, $CD4^+$ T cells were pretreated with 10 mmol/L methyl-β-cyclodextrin for 3 min to specifically deplete cholesterol from lipid rafts as previously described (26). Laurdan analysis revealed that the elevated GP values associated with IS formation (ΔGP = 0.195 $\pm$ 0.030, *fat-1* and 0.139 $\pm$ 0.015, WT, $n = 6–14$ cells per mouse for 1–2 mice per genotype) was diminished following methyl-β-cyclodextrin treatment (ΔGP = 0.053 $\pm$ 0.022, *fat-1* and 0.059 $\pm$ 0.033, WT), indicating that changes in the GP value at the IS are cholesterol-dependent.

In complementary experiments, GM1-specific microcluster recruitment was assessed using CTx-FITC. CTx has been used to mark membrane microdomains in the exofacial leaflet, although a significant fraction of GM1 is found outside l_o regions (30). Interestingly, in contrast to the enhanced l_o domain formation at the IS (Fig. 3*B*), GM1 recruitment was not altered in *fat-1* $CD4^+$ T cells (Fig. 3, *D* and *E*).

n-3 PUFA suppress the localization of signaling proteins into the IS

Following Ag recognition by the TCR, signaling cascades proximal to the IS are initiated by relocalization of a complex of molecules, i.e., protein kinases (Fyn, Lck, ZAP70, PLCγ-1), scaffolding proteins (LAT, Grb-2, SLP-76, CARMA1), and cytoskeletal proteins (F-actin) into the IS (5, 19, 31). In this study, the effect of

Downloaded from http://www.jimmunol.org/ by guest on January 29, 2022

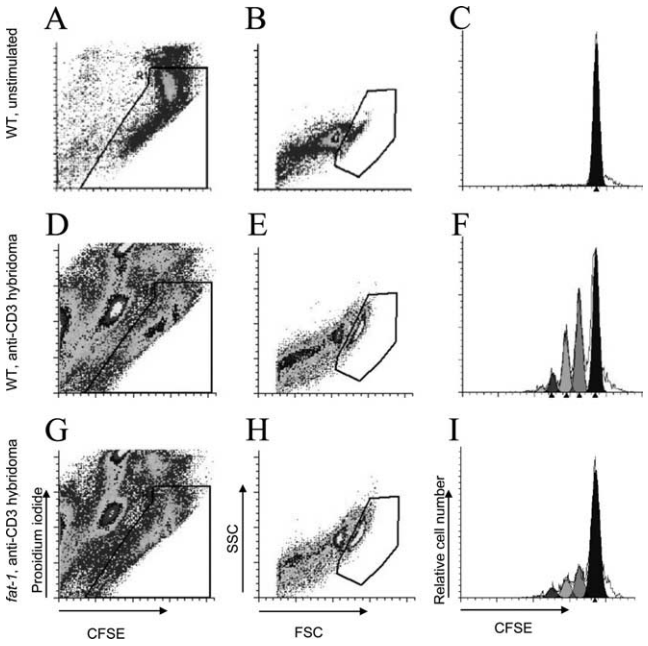

FIGURE 6. The effect of n-3 PUFA on lipid rafts and signaling protein activation associated with an alteration in T cell proliferation. Representative CFSE profiles of basal WT T cells (*A–C*), anti-CD3 hybridoma-stimulated WT (*D–F*), or *fat-1* CD4$^+$ T cells (*G–I*). Regions for viable cells (*A*, *D*, and *G*) and lymphocytes (*B*, *E*, and *H*) were set based on propidium iodide incorporation and forward and side scatter plots, respectively. Viable lymphocytes were defined as those events falling within both the viability and lymphocyte regions. Computer-aided modeling of each daughter generation (*C*, *F*, and *I*) was performed as described in *Materials and Methods*. The nondivided parental peak was obtained from the unstimulated control group (*C*). The left shift of peaks (*F* and *G*) indicated successive rounds of cell division.

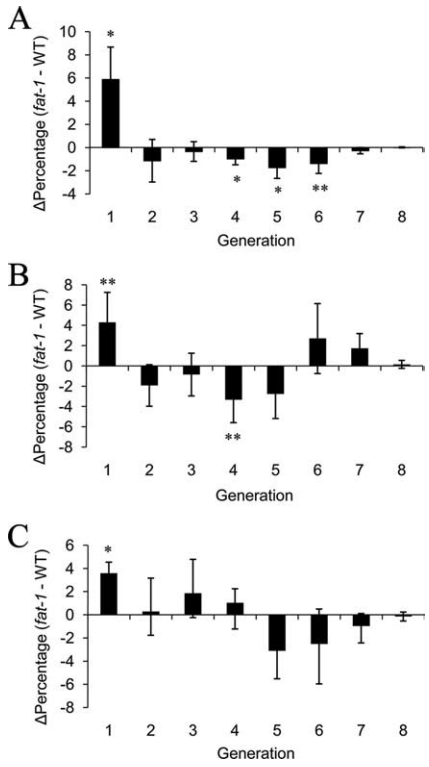

FIGURE 7. Examination of daughter cell generation shows suppressed *fat-1* CD4$^+$ T cell proliferation in response to stimulation. The difference in the percentage of T cells (Δpercentage) at each generation was obtained by subtracting the percentage of the WT group from the percentage of *fat-1*. Positive percentage data show that *fat-1* cultures had more cells in those generations, whereas negative data show fewer *fat-1* cells. Anti-CD3 hybridoma (*A*), anti-CD3/28 mAbs (*B*), and PMA/ionomycin (*C*) stimulated (n = 6–10 cultures from 3–5 mice per genotype for each stimulus). *, $p < 0.05$; **, $p < 0.10$.

n-3 PUFA on the localization of select signaling molecules in the plasma membrane at the IS was quantified. Fig. 4*A* shows representative cell images obtained following incubation with rabbit mAb specific to mouse LAT and the secondary Alexa Fluor 568 Ab specific to rabbit IgG. Relocalization of PKCθ, PLCγ-1, and F-actin into the IS, expressed as the percentage conjugate with patching, were suppressed in *fat-1* transgenic cells by 30% (p = 0.050), 32% (p = 0.081), and 36% (p = 0.020), respectively (Fig. 4*B*). In contrast, the intracellular localization of LAT and CARMA1 at the IS was not altered by n-3 PUFA.

n-3 PUFA down-regulate PLCγ-1 phosphorylation at the IS

Because phosphorylation of LAT and PLCγ-1 occurs at the very early stages of T cell activation, either phospho-LAT- or phospho-PLCγ-1-specific Ab was used to visualize the effect of n-3 PUFA on T cell activation. Specifically, the percentage conjugate patching of phospho-Y195 (LAT) (32) and phospho-Y783 (PLCγ-1) (33) was examined and showed that PLCγ-1 phosphorylation was suppressed by 29% (p = 0.034) in n-3 PUFA enriched cells at the IS, whereas LAT phosphorylation was not altered (p = 0.464) (Fig. 5).

n-3 PUFA suppress CD4$^+$ T cell proliferation

CD4$^+$ T cells were labeled with CFSE and cultured for 72 h for the purpose of determining whether the effect of n-3 PUFA on lipid rafts and signaling protein recruitment or activation was associated with an alteration in T cell proliferation. Using flow cytometry analysis, nonviable cells were gated out based on their uptake of propidium iodide (Fig. 6*A*, *D*, and *G*) and lymphocytes were identified by forward and side scatter plot analysis (Fig. 6, *B*, *E*, and *H*). The parental peak was obtained by examining unstimulated control cells, which did not divide (Fig. 6*C*), whereas cell division was visualized by the shift of CFSE peak to the left (11, 29). To identify each daughter generation, computer-aided modeling was performed (Fig. 6, *F* and *I*). Examination of the percentage of each daughter cell generation revealed that *fat-1* CD4$^+$ T cell proliferation was suppressed in response to anti-CD3 hybridoma stimulation. Specifically, a higher percentage of nondivided parental cells (Δpercentage = 5.87, p = 0.028) and lower percentage of daughter cells at generation 4 (Δpercentage = −0.98, p = 0.037), generation 5 (Δpercentage = −1.73, p = 0.042), and generation 6 (Δpercentage = −1.38, p = 0.065) were obtained (Fig. 7*A*). In addition, CD4$^+$ T cells stimulated by either anti-CD3/28 mAbs or PMA/ionomycin exhibited a similar trend; larger fraction at generation 1 (Δpercentage = 4.30, p = 0.085 anti-CD3/28 mAbs, Δpercentage = 3.58, p = 0.001 PMA/ionomycin) and a reduced number of cells at generation 4 (Δpercentage = −3.34, p = 0.081 anti-CD3/28 mAbs), suggesting a suppression of cell division in the *fat-1* group (Fig. 7, *B* and *C*).

In a complementary experiment, CD4$^+$ T cell proliferation was assessed by the incorporation of [^{3}H]thymidine. In accordance with CFSE profile data, thymidine uptake expressed as the proliferation index revealed that *fat-1* CD4$^+$ T cell division was significantly suppressed by 52% ($p < 0.001$), 45% (p = 0.002), and 56% (p = 0.001) in anti-CD3 hybridoma, anti-CD3/28 mAbs, and PMA/ionomycin stimulated cells, respectively (Fig. 8).

Downloaded from http://www.jimmunol.org/ by guest on January 29, 2022

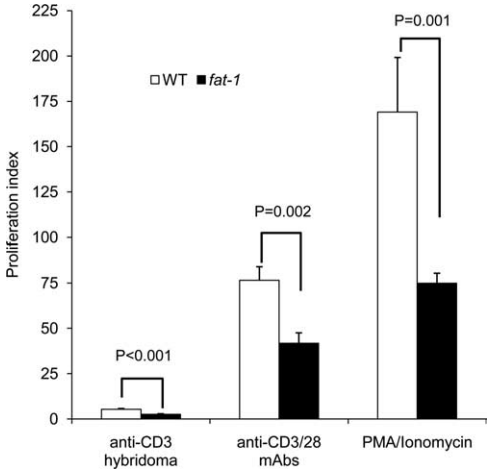

FIGURE 8. The proliferation of $CD4^+$ T cells in n-3 PUFA stimulation. The *fat-1* $CD4^+$ T cell proliferation was expressed as proliferation index using the formula (disintegrations per minute stimulated)/(disintegrations per minute unstimulated) in response to anti-CD3 hybridoma, anti-CD3/28 mAbs, or PMA/ionomycin stimulation ($n = 6–10$ cultures from 3–5 mice per genotype for each stimulus).

Discussion

It has been postulated that n-3 PUFA because of their perceived broad-acting effects on mammalian physiology, act at a fundamental level common to all cells, i.e., by altering the physical properties of biological membranes (9, 10, 18, 34–38). More specifically, we hypothesized that the anti-inflammatory effects of n-3 PUFA on $CD4^+$ T cells would be explained, in part, by suppressing or disrupting lipid raft formation at the IS.

To elucidate the membrane bioactive properties of n-3 PUFA in T cells, the *fat-1* transgenic mouse model was used because it is uniquely capable of converting n-6 PUFA to n-3 PUFA endogenously by introducing a *cis*-double bond into fatty acyl chains (24, 39). Data from initial experiments showed that the *fat-1* gene was functionally expressed in splenic $CD4^+$ T cells and that the plasma membrane was enriched in n-3 PUFA (Fig. 2).

We have demonstrated previously that n-3 PUFA suppress murine $CD4^+$ T cell proliferation by remodeling lipid raft fatty acid composition and by altering PKCθ colocalization (12). In that study, $CD4^+$ T cells were stimulated by culture plate-bound mAb to CD3 (anti-CD3 mAb) to induce the colocalization of PKCθ with GM1, a marker of lipid rafts. However, the direct visualization of lipid rafts at the IS is necessary to investigate microdomain assembly and localization at the plasma membrane. Hence, in the present study, we incubated $CD4^+$ T cells with Laurdan to directly measure membrane fluidity and visualize lipid rafts by two-photon microscopy. For this purpose, anti-CD3 hybridoma cells were used as APCs to form an IS because they express cell surface costimulatory B7 and ICAM-1 (27). In a major step toward developing a unifying mechanistic hypothesis addressing how dietary PUFA modulate cell membrane microdomains, we demonstrate for the first time to our knowledge that n-3 PUFA actually promote lipid raft formation at the IS (Fig. 3, *A–C*). These results can be explained in part by the fact that n-3 PUFA, specifically DHA, has a low affinity for cholesterol, providing a lipid-driven mechanism for lateral phase separation of cholesterol- or sphingolipid-rich lipid microdomains from the surrounding l_d phase (34–38). Hence, the insertion of DHA into the bulk membrane should enhance the coalescence of cholesterol-rich lipid raft-like domains in living cells. These findings are consistent with previous observations using immunogold electron microscopy of plasma membrane sheets coupled with spatial point analysis of validated microdomain markers (20). In that study, we demonstrated that DHA increased lipid raft clustering in HeLa cells, indicating that plasma membrane organization of inner leaflets is fundamentally altered by n-3 PUFA-enrichment.

With regard to the role of lipid rafts in T cell activation, T cells from patients with autoimmune disease synthesized more GM1 following TCR activation (5), suggesting that GM1-enriched domains play a critical role in the activation of immune responses. However, cholesterol overloading in healthy T cells reduced the lateral mobility of receptors and signaling molecules providing a link between plasma membrane cholesterol content and immunosenescence (5). These observations are controversial because GM1 and cholesterol, which are both thought to be lipid raft building blocks (3), play different roles in T cell activation and regulation. Therefore, we measured the recruitment of GM1 into the IS by labeling with CTx-FITC to evaluate the effect of n-3 PUFA on GM1-specific lipid rafts. Of interest, GM1 relocation as assessed by RRI was not altered by n-3 PUFA (Fig. 3*E*). This observation is consistent with a previous report in which GM1 localization as assessed by biochemical isolation of detergent-resistant membrane was not affected by PUFA treatment (40). Interestingly, the fatty acid composition of phospholipids in the exofacial leaflet of T cells, where GM1 is enriched, was not altered by n-3 PUFA (14). In addition, long chain PUFA are predominantly enriched in phospholipids localized to the cytofacial leaflet (14, 41). Based on these findings, the data suggest that the incorporation of n-3 PUFA into cytofacial leaflet phospholipids alters the lateral composition of lipid rafts in the plasma membrane, thereby altering the IS microenvironment to impact thresholds for the activation of TCR-mediated cell signaling.

The proximal events of cell signaling following Ag recognition by the TCR are initiated by the localization of signaling molecules into the IS (5). To evaluate the effect of n-3 PUFA on the localization of select signaling proteins, the percentage of cells with multiprotein signaling complexes relocalized to the IS was enumerated by immunofluorescence microscopy. Consistent with a perturbation in lipid raft structure, n-3 PUFA-enriched $CD4^+$ T cells exhibited a suppressed localization of PKCθ, PLCγ-1, and F-actin into the IS (Fig. 4). We also reported that PKCθ colocalization with GM1 in anti-CD3 mAb-stimulated T cells was suppressed by dietary fish oil and purified DHA ethyl ester administration (12). Although a significant fraction of GM1 can be found outside l_o regions (30, 42), the dislocation of PKCθ from GM1-enriched domains may explain in part why PKCθ accumulation at the IS was suppressed by n-3 PUFA, whereas lipid raft formation was enhanced. In addition, we also show that the localization of PLCγ-1 and F-actin was selectively suppressed by n-3 PUFA, whereas LAT and CARMA1 localization was not altered. In contrast, in a previous study, F-actin, LAT and PKCθ localization into the IS was not altered by n-3 PUFA (eicosapentaenoic acid) treatment compared with n-6 PUFA (arachidonic acid) (18). Indeed, both n-3 and n-6 PUFA treatment equally suppressed the localization of F-actin, talin, LFA-1α, LAT, and CD3ε into the IS, compared with the saturated stearic acid-treated (18:0) control group. The apparent differences between these studies may be attributed to the fact that Jurkat human T cells were directly incubated with 50 μmol/L fatty acid followed by antigenic stimulation (18).

Because not only the spatial migration but also the phosphorylation status of LAT and PLCγ-1 is critical for T cell activation (32, 33) and dietary fish oil has been shown to modulate PLCγ-1 phosphorylation in rat lymphocytes (43), we counted cells with phospho-specific immunofluorescent patching to assess the activation status of those proteins. In accordance with the localization results, LAT phosphorylation was not affected by n-3 PUFA, but

Downloaded from http://www.jimmunol.org/ by guest on January 29, 2022

PLCγ-1 phosphorylation was suppressed in *fat-1* transgenic T cells (Fig. 5). These data indicate that n-3 PUFA selectively modulate the localization or activation status of signaling proteins in TCR-mediated T cell activation.

The function of the IS is still evolving. For example, membrane condensation and signaling protein translocation to the IS has been shown to be critical for TCR-triggered T cell activation (21). In contrast, compelling data suggest central supramolecular activation cluster of mature IS may promote TCR/CD3 internalization and recycling (44). In addition, TCR microclusters initiate T cell signaling in seconds (45) following binding to peptide-MHC complex, but the signal becomes weaker when central supramolecular activation cluster is formed in minutes (46, 47). These observations suggest that the dynamic nature of the IS and perhaps rapid formation or dissolution of rafts promote TCR signaling. It is possible, therefore, that n-3 PUFA by stabilizing lipid rafts at the IS disrupt lipid-protein interactions and perturb membrane structure or function.

Alteration of $CD4^+$ T cell lipid raft microdomains and proximal T cell signaling by n-3 PUFA in *fat-1* cells resulted in the suppression of proliferation (Figs. 7*A* and 8), indicating the critical importance of lipid raft localization of proteins such as PKCθ, PLCγ-1, and F-actin to TCR signaling. To test whether the mechanism of suppression by n-3 PUFA was limited to the IS or proximal signaling cascades, T cells were stimulated with either anti-CD3/28 mAbs or PMA/ionomycin to bypass IS formation and TCR-mediated signaling, respectively. T cell proliferation by anti-CD3/28 mAbs and PMA/ionomycin was suppressed as assessed by CFSE profiles and thymidine uptake, indicating that the down-regulation of T cell proliferation by n-3 PUFA is not limited to TCR-mediated activation. Indeed, CFSE profile analysis revealed that the largest difference in the percentage was associated with the nondividing parental generation when T cells were stimulated with the IS forming anti-CD3 hybridoma cell model (Fig. 7), consistent with a very strong suppression of T cell proliferation. These data are consistent with previous reports that n-3 PUFA are anti-inflammatory and immunomodulatory in vivo (12, 48).

In general, hyperactivation of $CD4^+$ T cells is associated with enhanced susceptibility to autoimmune disorders and chronic inflammatory diseases induced diseases (9, 10). Recently, our lab reported that *fat-1* mice exhibited an enhanced ability to resolve dextran sodium sulfate-induced intestinal inflammation and injury (25). Because subsets of $CD4^+$ T cells are known to be critical mediators of chronic inflammation, results from our study may partially explain why n-3 PUFA favorably modulate the inflammation-dysplasia-carcinoma axis.

In conclusion, we have shown that n-3 PUFA promote the formation of lipid rafts and perturb the reorganization of signaling machinery that is critical to T cell activation. These results provide a critical new paradigm in understanding the molecular mechanisms through which dietary n-3 PUFA modulate T cell activation. Additional studies are needed to further elucidate the effect of dietary n-3 PUFA on T cell signaling networks.

Acknowledgments

We thank J. X. Kang (Department of Medicine, Harvard University) for providing *fat-1* breeder mice and L. Zhou for statistical assistance.

Disclosures

The authors have no financial conflict of interest.

References

1. Singer, S. J., and G. L. Nicolson. 1972. The fluid mosaic model of the structure of cell membranes. *Science* 175: 720–731.
2. Lingwood, D., and K. Simons. 2007. Detergent resistance as a tool in membrane research. *Nat. Protoc.* 2: 2159–2165.
3. Pike, L. J. 2004. Lipid rafts: heterogeneity on the high seas. *Biochem. J.* 378: 281–292.
4. Hanzal-Bayer, M. F., and J. F. Hancock. 2007. Lipid rafts and membrane traffic. *FEBS Lett.* 581: 2098–2104.
5. Jury, E. C., F. Flores-Borja, and P. S. Kabouridis. 2007. Lipid rafts in T cell signalling and disease. *Semin. Cell Dev. Biol.* 18: 608–615.
6. Brassard, P., A. Larbi, A. Grenier, F. Frisch, C. Fortin, A. C. Carpentier, and T. Fulop. 2007. Modulation of T-cell signalling by non-esterified fatty acids. *Prostaglandins Leukot. Essent. Fatty Acids* 77: 337–343.
7. Sijben, J. W., and P. C. Calder. 2007. Differential immunomodulation with long-chain n-3 PUFA in health and chronic disease. *Proc. Nutr. Soc.* 66: 237–259.
8. Siddiqui, R. A., K. A. Harvey, G. P. Zaloga, and W. Stillwell. 2007. Modulation of lipid rafts by omega-3 fatty acids in inflammation and cancer: implications for use of lipids during nutrition support. *Nutr. Clin. Pract.* 22: 74–88.
9. Chapkin, R. S., L. A. Davidson, L. Ly, B. R. Weeks, J. R. Lupton, and D. N. McMurray. 2007. Immunomodulatory effects of (n-3) fatty acids: putative link to inflammation and colon cancer. *J. Nutr.* 137: 200S–204S.
10. Chapkin, R. S., D. N. McMurray, and J. R. Lupton. 2007. Colon cancer, fatty acids and anti-inflammatory compounds. *Curr. Opin. Gastroenterol.* 23: 48–54.
11. Zhang, P., W. Kim, L. Zhou, N. Wang, L. H. Ly, D. N. McMurray, and R. S. Chapkin. 2006. Dietary fish oil inhibits antigen-specific murine Th1 cell development by suppression of clonal expansion. *J. Nutr.* 136: 2391–2398.
12. Fan, Y. Y., L. H. Ly, R. Barhoumi, D. N. McMurray, and R. S. Chapkin. 2004. Dietary docosahexaenoic acid suppresses T cell protein kinase C theta lipid raft recruitment and IL-2 production. *J. Immunol.* 173: 6151–6160.
13. Li, Q., L. Tan, C. Wang, N. Li, Y. Li, G. Xu, and J. Li. 2006. Polyunsaturated eicosapentaenoic acid changes lipid composition in lipid rafts. *Eur. J. Nutr.* 45: 144–151.
14. Fan, Y. Y., D. N. McMurray, L. H. Ly, and R. S. Chapkin. 2003. Dietary (n-3) polyunsaturated fatty acids remodel mouse T-cell lipid rafts. *J. Nutr.* 133: 1913–1920.
15. Zachowski, A. 1993. Phospholipids in animal eukaryotic membranes: transverse asymmetry and movement. *Biochem. J.* 294(Pt. 1): 1–14.
16. Chow, S. C., L. Sisfontes, M. Jondal, and I. Bjorkhem. 1991. Modification of membrane phospholipid fatty acyl composition in a leukemic T cell line: effects on receptor mediated intracellular Ca^{2+} increase. *Biochim. Biophys. Acta* 1092: 358–366.
17. Sasaki, T., Y. Kanke, K. Kudoh, Y. Misawa, J. Shimizu, and T. Takita. 1999. Effects of dietary docosahexaenoic acid on surface molecules involved in T cell proliferation. *Biochim. Biophys. Acta* 1436: 519–530.
18. Geyeregger, R., M. Zeyda, G. J. Zlabinger, W. Waldhausl, and T. M. Stulnig. 2005. Polyunsaturated fatty acids interfere with formation of the immunological synapse. *J. Leukocyte Biol.* 77: 680–688.
19. Tanner, M. J., W. Hanel, S. L. Gaffen, and X. Lin. 2007. CARMA1 coiled-coil domain is involved in the oligomerization and subcellular localization of CARMA1 and is required for T cell receptor-induced NF-κB activation. *J. Biol. Chem.* 282: 17141–17147.
20. Chapkin, R. S., N. Wang, Y. Y. Fan, J. R. Lupton, and I. A. Prior. 2008. Docosahexaenoic acid alters the size and distribution of cell surface microdomains. *Biochim. Biophys. Acta* 1778: 466–471.
21. Gaus, K., E. Chklovskaia, B. Fazekas de St Groth, W. Jessup, and T. Harder. 2005. Condensation of the plasma membrane at the site of T lymphocyte activation. *J. Cell Biol.* 171: 121–131.
22. Gaus, K., T. Zech, and T. Harder. 2006. Visualizing membrane microdomains by Laurdan 2-photon microscopy. *Mol. Membr. Biol.* 23: 41–48.
23. Rentero, C., T. Zech, C. M. Quinn, K. Engelhardt, D. Williamson, T. Grewal, W. Jessup, T. Harder, and K. Gaus. 2008. Functional implications of plasma membrane condensation for T cell activation. *PLoS ONE* 3: e2262.
24. Kang, J. X., J. Wang, L. Wu, and Z. B. Kang. 2004. Transgenic mice: *fat-1* mice convert n-6 to n-3 fatty acids. *Nature* 427: 504.
25. Jia, Q., J. R. Lupton, R. Smith, B. R. Weeks, E. Callaway, L. A. Davidson, W. Kim, Y. Y. Fan, P. Yang, R. A. Newman, et al. 2008. Reduced colitis-associated colon cancer in *fat-1* (n-3 fatty acid desaturase) transgenic mice. *Cancer Res.* 68: 3985–3991.
26. Zidovetzki, R., and I. Levitan. 2007. Use of cyclodextrins to manipulate plasma membrane cholesterol content: evidence, misconceptions and control strategies. *Biochim. Biophys. Acta* 1768: 1311–1324.
27. Tamir, A., M. D. Eisenbraun, G. G. Garcia, and R. A. Miller. 2000. Age-dependent alterations in the assembly of signal transduction complexes at the site of T cell/APC interaction. *J. Immunol.* 165: 1243–1251.
28. Tavano, R., R. L. Contento, S. J. Baranda, M. Soligo, L. Tuosto, S. Manes, and A. Viola. 2006. CD28 interaction with filamin-A controls lipid raft accumulation at the T-cell immunological synapse. *Nat. Cell Biol.* 8: 1270–1276.
29. Quah, B. J., H. S. Warren, and C. R. Parish. 2007. Monitoring lymphocyte proliferation in vitro and in vivo with the intracellular fluorescent dye carboxyfluorescein diacetate succinimidyl ester. *Nat. Protoc.* 2: 2049–2056.
30. Owen, D. M., M. A. Neil, P. M. French, and A. I. Magee. 2007. Optical techniques for imaging membrane lipid microdomains in living cells. *Semin. Cell Dev. Biol.* 18: 591–598.
31. Gaide, O., B. Favier, D. F. Legler, D. Bonnet, B. Brissoni, S. Valitutti, C. Bron, J. Tschopp, and M. Thome. 2002. CARMA1 is a critical lipid raft-associated regulator of TCR-induced NF-κB activation. *Nat. Immunol.* 3: 836–843.
32. Reynolds, L. F., C. de Bettignies, T. Norton, A. Beeser, J. Chernoff, and V. L. Tybulewicz. 2004. Vav1 transduces T cell receptor signals to the activation

Downloaded from http://www.jimmunol.org/ by guest on January 29, 2022

of the Ras/ERK pathway via LAT, Sos, and RasGRP1. *J. Biol. Chem.* 279: 18239–18246.
33. Moore, A. L., M. W. Roe, R. F. Melnick, and S. D. Lidofsky. 2002. Calcium mobilization evoked by hepatocellular swelling is linked to activation of phospholipase Cγ. *J. Biol. Chem.* 277: 34030–34035.
34. Shaikh, S. R., and M. Edidin. 2006. Polyunsaturated fatty acids, membrane organization, T cells, and antigen presentation. *Am. J. Clin. Nutr.* 84: 1277–1289.
35. Shaikh, S. R., and M. A. Edidin. 2006. Membranes are not just rafts. *Chem. Phys. Lipids* 144: 1–3.
36. Shaikh, S. R., V. Cherezov, M. Caffrey, W. Stillwell, and S. R. Wassall. 2003. Interaction of cholesterol with a docosahexaenoic acid-containing phosphatidylethanolamine: trigger for microdomain/raft formation? *Biochemistry* 42: 12028–12037.
37. Wassall, S. R., and W. Stillwell. 2008. Docosahexaenoic acid domains: the ultimate non-raft membrane domain. *Chem. Phys. Lipids* 153: 57–63.
38. Soni, S. P., D. S. LoCascio, Y. Liu, J. A. Williams, R. Bittman, W. Stillwell, and S. R. Wassall. 2008. Docosahexaenoic acid enhances segregation of lipids between raft and nonraft domains: ^{2}H-NMR study. *Biophys. J.* 95: 203–214.
39. Ma, D. W., V. Ngo, P. S. Huot, and J. X. Kang. 2006. N-3 polyunsaturated fatty acids endogenously synthesized in *fat-1* mice are enriched in the mammary gland. *Lipids* 41: 35–39.
40. Stulnig, T. M., M. Berger, T. Sigmund, D. Raederstorff, H. Stockinger, and W. Waldhausl. 1998. Polyunsaturated fatty acids inhibit T cell signal transduction by modification of detergent-insoluble membrane domains. *J. Cell Biol.* 143: 637–644.
41. Pike, L. J., X. Han, and R. W. Gross. 2005. Epidermal growth factor receptors are localized to lipid rafts that contain a balance of inner and outer leaflet lipids: a shotgun lipidomics study. *J. Biol. Chem.* 280: 26796–26804.
42. Blank, N., M. Schiller, S. Krienke, G. Wabnitz, A. D. Ho, and H. M. Lorenz. 2007. Cholera toxin binds to lipid rafts but has a limited specificity for ganglioside GM1. *Immunol. Cell Biol.* 85: 378–382.
43. Sanderson, P., and P. C. Calder. 1998. Dietary fish oil appears to prevent the activation of phospholipase C-γ in lymphocytes. *Biochim. Biophys. Acta* 1392: 300–308.
44. Lee, K. H., A. R. Dinner, C. Tu, G. Campi, S. Raychaudhuri, R. Varma, T. N. Sims, W. R. Burack, H. Wu, J. Wang, et al. 2003. The immunological synapse balances T cell receptor signaling and degradation. *Science* 302: 1218–1222.
45. Huse, M., L. O. Klein, A. T. Girvin, J. M. Faraj, Q. J. Li, M. S. Kuhns, and M. M. Davis. 2007. Spatial and temporal dynamics of T cell receptor signaling with a photoactivatable agonist. *Immunity* 27: 76–88.
46. Mossman, K. D., G. Campi, J. T. Groves, and M. L. Dustin. 2005. Altered TCR signaling from geometrically repatterned immunological synapses. *Science* 310: 1191–1193.
47. Varma, R., G. Campi, T. Yokosuka, T. Saito, and M. L. Dustin. 2006. T cell receptor-proximal signals are sustained in peripheral microclusters and terminated in the central supramolecular activation cluster. *Immunity* 25: 117–127.
48. Ly, L. H., R. Smith, III, R. S. Chapkin, and D. N. McMurray. 2005. Dietary n-3 polyunsaturated fatty acids suppress splenic $CD4^{+}$ T cell function in interleukin (IL)-$10^{-/-}$ mice. *Clin. Exp. Immunol.* 139: 202–209.

Downloaded from http://www.jimmunol.org/ by guest on January 29, 2022